Heliyon 10 (2024) e34008

Contents lists available at ScienceDirect

Heliyon

journal homepage: www.cell.com/heliyon

Research article

SHP2 mediates the ROS/JNK/NFAT4 signaling pathway in gastric cancer cells prompting lncRNA SNHG18 to drive gastric cancer growth and metastasis via CAR-T cells

Lin An [1], Yue Huo [1], Na Xiao, Shenyong Su, Kunjie Wang [*]

Department of Medical Oncology, Affiliated Hospital of Hebei University, Hebei Key Laboratory of Cancer Radiotherapy and Chemotherapy, Baoding, Hebei, 071000, PR China

ARTICLE INFO

Keywords:
Gastric cancer
SHP2
ROS/JNK/NFAT4 signaling pathway
CAR-T cells
miR-211-5p/BRD4 axis

ABSTRACT

Objective: In gastric cancer cells, the influence of CAR T cells can be produced in the process of inhibiting the progression of gastric cancer, and the role of tyrosine phosphatase SHP2 can be explored in this study, along with its molecular mechanisms. Methods: The research utilized subcutaneous tumor models in nude mice to assess gastric cancer progression. Protein expression was detected using Western blotting, while Q-PCR examined the expression levels of lncRNA SNHG18 and miR-211-5p in MGC-803 cells. The relationship between miR-211-5p and lncRNA SNHG18 can be analyzed by dual luciferase reporter genes. The migratory ability of MGC-803 cells was determined through wound healing and transwell experiments, and cell proliferation was evaluated using a CCK-8 assay.Results: SHP2 was found to inhibit the cytotoxic effects of CAR-T cells on MGC-803 cells, and it suppressed the expression of proteins related to the ROS/JNK/NFAT4 signaling pathway in MGC-803 cells and the miR-211-5p/BRD4 axis in CAR-T cells. In addition, the proliferation, invasion and migration of MGC-803 cells were promoted, and the expression of miR-211-5p could be inhibited specifically by ncRNA SNHG18, as shown below: SHP2 in gastric cancer cells mediates the ROS/JNK/NFAT4 signaling pathway and induces lncRNA SNHG18, which, through the miR-211-5p/BRD4 axis in CAR-T cells, promotes gastric cancer growth and metastasis.

1. Introduction

As a malignancy, gastric cancer (GC) is responsible for a significant global burden, fifth in its global incidence ranking, third in its mortality ranking, GC is prevalent, particularly in East Asia, which has the highest incidence of the disease.The incidence and mortality of gastric cancer rank second and third respectively in China, and the burden is lower in cities than in rural areas.East and Southwest China record the highest numbers in incidence and mortality, with provinces like Qinghai, Anhui, Fujian, and Gansu having higher age-standardized mortality rates. *Helicobacter pylori* infection is one of the risk factors for gastric cancer, EB virus infection, genetic factors, environmental factors, and lifestyle habits, such as a high-salt diet, low fruit intake, smoking, and alcohol abuse.In recent

* Corresponding author. Department of Medical Oncology, Affiliated Hospital of Hebei University, Hebei Key Laboratory of Cancer Radiotherapy and Chemotherapy, Baoding, Hebei, 071000, PR China.
E-mail address: wkj20231009@163.com (K. Wang).
[1] These authors share first authorship.

https://doi.org/10.1016/j.heliyon.2024.e34008
Received 29 March 2024; Received in revised form 1 July 2024; Accepted 2 July 2024
Available online 6 July 2024

years, advances in local resection and early screening have improved the 5-year survival rate for gastric cancer. Typical treatment methods vary, depending on the stage, and include endoscopic resection, open gastrectomy, minimally invasive surgery (laparoscopy, robotics), chemotherapy, radiotherapy, targeted therapy, and immunotherapy [1–3]. However, advanced stage is the time when patients are diagnosed, and recurrence or metastasis of cancer is common after surgery or first-line treatment. Hence, molecular targeted therapy and immunotherapy are extensively researched.

Src Homology 2 Domain Containing Tyrosine Phosphatase-2 is the full name of SHP2, which is encoded by the PTPN11 gene, a non-receptor tyrosine phosphatase, is involved in regulating several cellular signaling pathways, activation of cell adhesion molecules, cytokine receptors, and growth factor receptors are included in the cell. It plays a vital role in the growth, differentiation, and apoptosis of normal cells and tissues. However, its activity can become aberrant in various types of cancers, including gastric cancer, where it may indirectly promote tumor growth and survival by activating signaling pathways like RAS/MAPK. This indicates that it could have a contributing effect on tumor development and progression [4–6]. Theoretically, inhibiting SHP2's activity could disrupt cancer cell signaling and inhibit their proliferation, representing a potential anti-cancer therapy.

In order for cancer cells to recognize and attack, as a treatment, patients' T cells can be reprogrammed with CAR-T cell therapy. Among the treatments, its success has been seen in blood cancers such as diffuse large B-cell lymphoma (DLBCL) and acute lymphoblastic leukemia (ALL). However, for the treatment of gastric cancer, the research and clinical trial phase is where CAR T-cell therapy is at, with researchers trying to identify specific antigens suitable for targeting gastric cancer and optimizing the CAR-T cell therapy [7,8]. Potential target antigens on gastric cancer cells may include HER2, CEA, EGFR, and others, but these are not unique to gastric cancer and may also be expressed on normal cells, adding complexity and potential side effects to Stomach cancer can be treated with CAR-T therapy, and several challenges are applied by CAR-T therapy during the treatment of solid tumors, such as ensuring that CAR-T cells reach the tumor microenvironment, penetrate the dense arrangement of tumor cells, and overcome the immunosuppressive environment caused by the tumor. Based on these studies, we hypothesize that the SHP2 produced in gastric cancer can suppress the toxicity of CAR-T cells against gastric cancer cells, thereby accelerating gastric cancer progression [9,10]. In vivo and in vitro experiments were designed to analyze how CAR T cell inhibition of gastric cancer progression is influenced by the tyrosine phosphatase SHP2 in gastric cancer cells.

2. Methods

2.1. Bioinformatics analysis

In carrying out the process of analysis, NCBI the GEO database on the platform can be used (http://www.ncbi.nlm.nih.gov/geo/), which, in turn, make to the identification of gene chip, particularly those related to gastric cancer mRNA datasets. These datasets underwent normalization and differential expression analysis using R (version 4.1.3) and relevant packages, including the Limma R package. Differentially expressed genes (DEGs) are shown in this way, and visualizations can be shown through heat maps as well as volcano maps.The criteria for identifying DEGs were set at $|\log FC| > 1$ and $p < 0.05$. Likewise, gastric cancer-related lncRNA datasets were downloaded and analyzed to find differentially expressed lncRNAs (DELs).

For further analysis of the identified genes, the Genome Encyclopedia (KEGG) and AVID Gene Ontology (GO) bioinformatics resource database can be used.This analysis identified gene clusters and pathways exhibiting biological differences between gastric cancer and normal tissues. Scatterplot of KEGG enrichment analysis and bar plot of GO enrichment analysis can be used by creating GO enrichment analysis for ggplot2 software package.

The starBase database was used to predict lncRNAs associated with differentially expressed mRNAs (DEMs), with interaction site maps constructed accordingly. In addition, normal tissue and gastric cancer data can be downloaded from UCSC Xena (https://xenabrowser.net/), whose analysis was performed in R(version 4.1.3).This analysis produced scatter plots of co-expression for individual genes and box plots comparing expression levels between disease and normal tissues.

2.2. Cell culture and transfection

The company was the source of CAR T cells and the human gastric cancer cell line MGC-803. rmi-1640 of 1 % penicillin-streptomycin solution and 10 % fetal bovine serum were contained in MGC-803 cells, which were cultured in a three-gas incubator containing 1 % O2. In the experiment, the selected cells were in a logarithmic growth phase, and the density of $1 \times 10\hat{}5$ cells per well could be cultured in a 6-well plate. 60 % is the number where convergence is achieved.

The negative control, LncRNA SNHG18 sh-RNA and SHP2 sh-RNA were synthesized by Sangon Biotechnology. Sigma-Aldrich obtained miR-211-5p mimics and SHP2 mimics, Thermer Fisher Technologies obtained miR-211-5p inhibitors, These constructs can be transfected by the use of Lipofectamine 3000 (Thermo Fisher Scientific). After 6 h, the complete medium can be replaced by the medium, and the following groups are divided into cells: SHP2-NC, SHP2-NC + CAR-T cells, SHP2-mimic, SHP2-mimic + CAR-T cells, NC, lncRNA SNHG18 sh-RNA, NC + miR-211-5p-inhibitor, lncRNA SNHG18 sh-RNA + miR-211-5p-inhibitor, NC + miR-211-5p-mimic, and lncRNA SNHG18 sh-RNA + miR-211-5p-mimic groups. Additionally, PHPS1 (a SHP2 inhibitor, 30 μmol/L) was added to a batch of SHP2-NC and SHP2-mimic MGC-803 cells, to serve as SHP2-NC + PHPS1 and SHP2-mimic + PHPS1 groups.

2.3. Co-culture of cells

A cytokine free RPMI-1640 medium can be used, and MGC-803 cells can be inoculated with a $1 \times 10\hat{}6$ cell/pore density.After four

days, CAR-T cells were introduced into the transwell chambers, without any additional exogenous cytokines in the medium. Through overnight incubation, the medium can be extracted from culture plates as well as transwell chambers. The lower cavity of the transwell system can be added via fresh media. The transwell chamber needs to be reinserted and incubated for 48 h before continuing testing. The transwell chamber needs to be removed after incubation and the medium can be aspirated in a cell culture plate. After two washes with PBS, residual cells and media are eliminated. Further analysis can be fixed by 4 % paraformaldehyde.

2.4. Subcutaneous tumorigenesis in nude mice

Henan Sibex Biotechnology Co., Ltd. purchased BALB/c male nude mice, a total of 25, 6 weeks old, SPF grade. They were housed in a SPF grade, constant temperature and humidity clean room, using individually ventilated cage systems (IVC), four mice per cage. The temperature/humidity was controlled at (26 ± 2)°C/40–60 %, with a light/dark cycle of 12h/12h. The mice had access to autoclaved SPF-grade food and ultrafiltered purified water. MGC-803 cells of logarithmic growth can be collected at a concentration of 2 × 105/mL where cell suspension is regulated, digested by pancreatic enzymes, and washed by PBS. The cell suspension was injected subcutaneously into the nude mice; care was taken to insert the needle about 1 cm under the skin and slide it left and right subcutaneously to facilitate the formation of a cell mass and reduce spillage of the cell suspension from the needle hole after injection. The ethics committee of Hebei University Hospital approved the study.(HDFYLL-KGCP-2024-091)

2.5. Q-PCR

Total RNA of MGC-803 cells was extracted by TRIzol reagent, and cDNA could be synthesized by reverse transcription kit. The TaqMan reverse transcription kit can be used (N8080234, Thermo Fisher), and quantitative PCR (qPCR) can be performed on the Bio-Rad real-time detection system. In the PCR scheme, denaturation is first performed for 3 min at 95 °C, then for 5 s, annealing for 10 s is performed at 56 °C, and 40 cycles of 25 s are extended at 72 °C. Primers used were as follows: lncRNA SNHG18 (F: 5′-CCTAATGC-TAAACATTGGTACA-3′, R: 5′-GCAACACAGCATCACCTGTAC-3′), miR-211-5p (F: 5′-ACACTCCAGCTGGGCAAGTAGCATCAACTA-3′, R: 5′-TGGTGTCGTGGAGTCG-3′), and GAPDH (F: 5′-TCAACGGCACAGTCAAGG-3′, R: 5′-TCAACGGCACAGTCAAGG-3′). Results were analyzed using the 2-ΔΔCt method.

2.6. The assay of Dual-Luciferase reporter

Dual-luciferase reporter plasmids, designated as SNHG18-wt and SNHG18-mut, were constructed using the geneses enzyme labeling system. For the luciferase assay, After 48 h, the dual luciferase reporter gene test system can be used and the dual luciferase activity can be measured using the manufacturer's protocol. The simulated negative control (NC) and MGC-803 cells can be used together to cotransfect SNHG18-wt or SNHG18-mut.

2.7. Scratch assay

The 6-well plate can be inoculated with MGC-803 cells, and if complete confluence is achieved, the vertical scratch can be made through the pipette tip at the bottom of the plate. The old medium can be removed and the isolated cell fragments can be washed through sterile PBS. Images were taken of three random fields of view under an inverted microscope, designated as 0 h. Subsequently, Under an inverted microscope, cell migration at 0 h was observed and photographed. DMEM medium can be added per well, 48 h is the time for reincubation, and the mean distance between cells was calculated.

2.8. Transwell assay

Trypsin digestion can be used by log-grown MGC-803 cells, and after 24 h of application, trypsin digestion cells can be used, and the cells can be treated by the experimental group, resuspended in serum-free DMEM, and a cell suspension was prepared. 200 μL of cell suspension containing 8 × 10^4 cells can be added, 50 μL of serum-free DMEM can be added in the upper chamber of the Transwell system, and 1 h is the time of placement in the cell incubator. 20 % fetal bovine serum medium 600 μL can be added to the lower chamber, 24 h is the time for reincubation. In 4 % paraformaldehyde, 30 min is the fixed time, tap water can be washed, 30 min is 0.1 % crystal violet staining time, and cells that do not migrate through the membrane can be wiped away by a cotton swab. Migrating cells can be viewed under an inverted microscope, photography can be performed, and three different fields of view can be randomly selected.

2.9. Cell counting Kit-8 (CCK-8)

Cell suspensions can be prepared in a whole culture medium with a density of 5 × 10^4/mL. Counting can be performed by using cell counting plates, digestion, and dilution can be performed in log-grown MGC-803 cells. After cell adhesion, 24 and 48 h are the time of cultivation, respectively. 100 μL suspension can be added to each hole of the 96-well plate and incubated at 37 °C with 5 % CO2. 100 μL fresh complete medium can be replaced with old medium, CCK-8 reagent 10 μL is added per well, 2 h is its incubation time in the dark, at 450 nm, cell viability can be measured by the use of an enzyme-linked immunoassay.

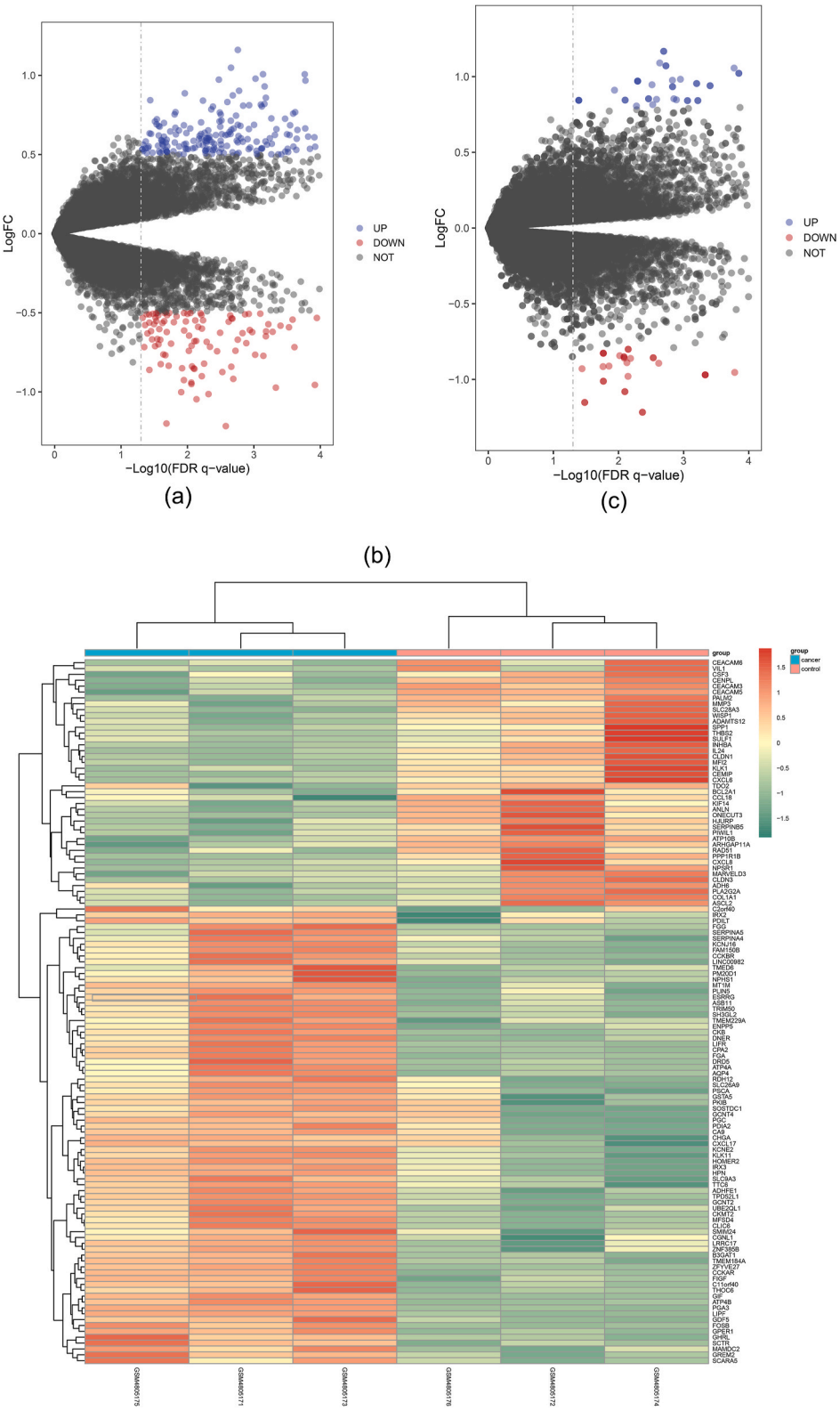

Fig. 1. Results of bioinformatics analysis.
A: The ggplot2 software package constructs a volcanic map of the dataset GSE109476 in R software for visual grouping of differential genes (DEGs); B:R software package pheatmap to draw a heat map of DEG cluster analysis; C: ggplot2 software package constructs a volcanic map of the dataset

GSE109476 in R software. D:R software package pheatmap to plot the cluster analysis heat map of DEG; E: GO pathway map of up-regulated differentially expressed genes; F: GO pathway diagram of down-regulated DEGs; G: KEGG enrichment analysis map was plotted using the R language ggplot2 package; H: association site of has-miR-211-5p and BRD4; I: Site map of SNHG18 and has-miR-211-5p; J-N: Correlation scatter plots were plotted for PTPN11 and MAPK8, SOD1 and MAPK8, SOD1 and PTPT11, MAPK8 and NFAT4, MAPK8 and JUN; O: Expression of PTPTN11 in tumor tissue and in adjacent tissues.

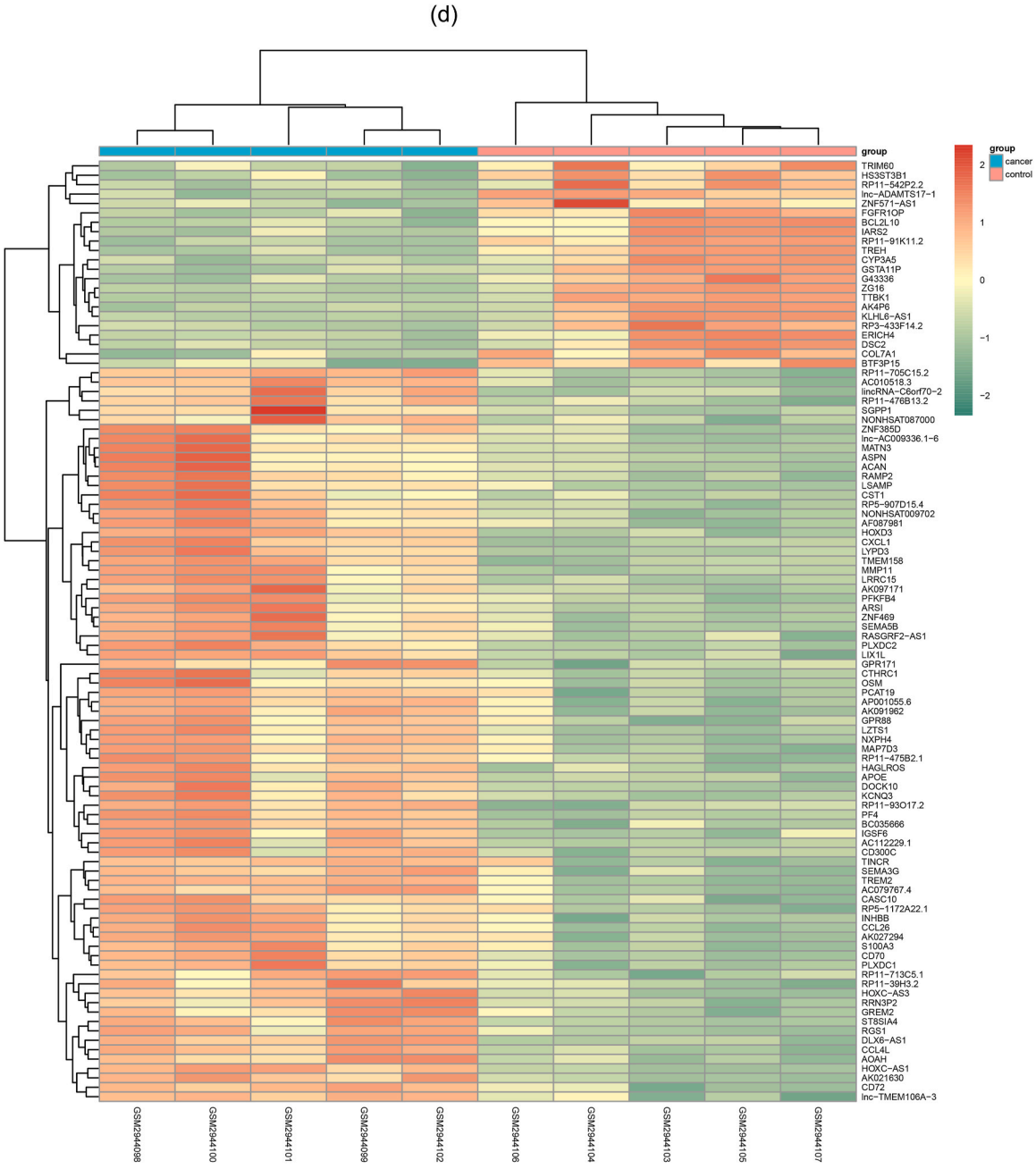

Fig. 1. (*continued*).

2.10. Western blot

TSDS-PAGE can separate each sample protein (10 μg), the PVDF membrane is transferred, 2 h is blocked by 5 % skim milk, and the primary antibody is added. Total protein can be extracted by RIPA cracking buffer, BCA protein assay kit can be used by each group of protein samples, and quantification can be carried out, followed by secondary antibodies conjugated with HRP anti-rabbit IgG (ab288151, 1:2000). ECL color-developing agent was then added for exposure and imaging. The gray values of protein bands can be

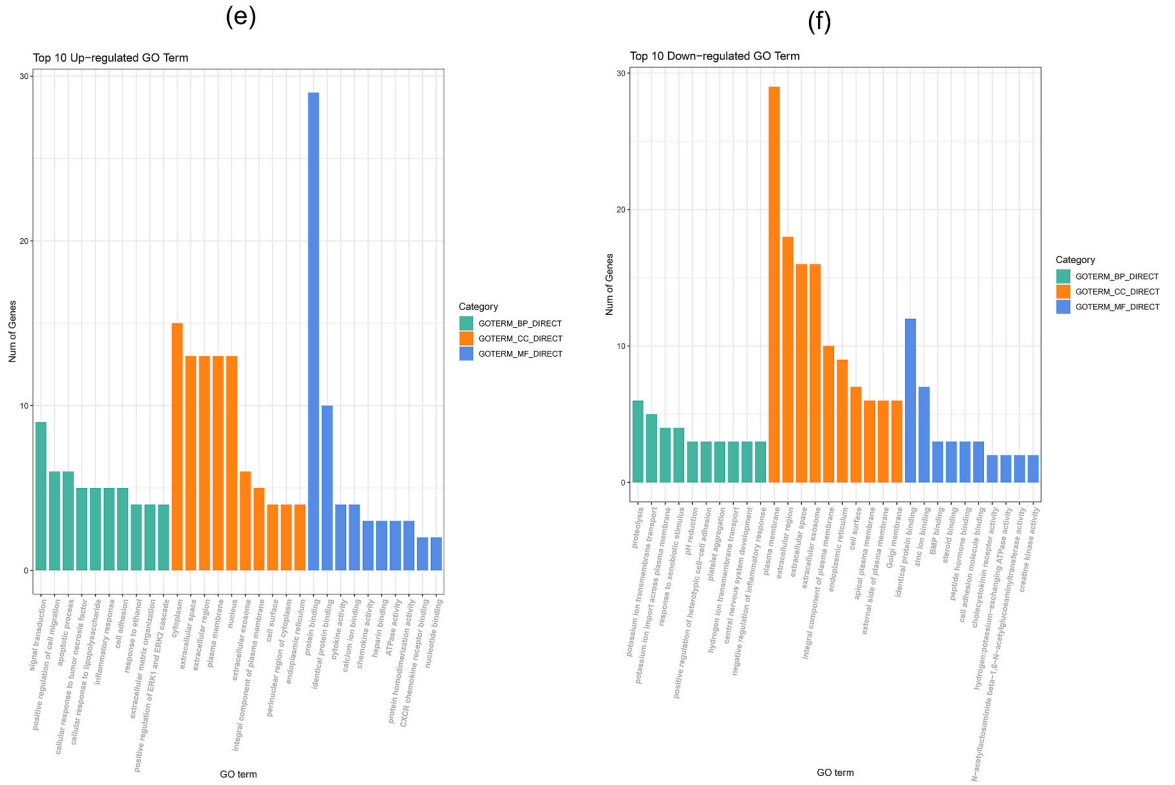

Fig. 1. (*continued*).

analyzed by using ImageJ software.

2.11. The analysis of statistic

During the use of GraphPad Prism 9.0, data analysis and processing can be carried out. Mean ± standard deviation (SD) can be expressed as measured data. When the two groups of data are compared, the independent sample T-test can be used, and the statistical significance can be shown when the p value is < 0.05.

3. Results

3.1. Results of bioinformatics analysis

Investigated gastric cancer-related datasets in the GEO database and obtained the GSE109476 gene expression dataset for gastric cancer mRNA. This dataset, using the Agilent-076500 Human lncRNA + mRNA array platform (Probe name version) with probe GPL22755, was normalized via quantile normalization using the R language limma package. It comprised three cancerous and three normal tissues. Differential gene analysis was carried out (|logFC|>1, p-value<0.05). A volcano plot (Fig. 1A) and a heatmap for DEG clustering analysis (Fig. 1B) were created using the ggplot2 and pheatmap packages in R, respectively.

Another dataset for gastric cancer-related mRNA, GSE109476, was downloaded from the Arraystar Human LncRNA microarray V2.0 platform with probe GPL24530. This data is also normalized using the limma package. It included five cancerous and five non-cancerous tissues. The differential gene analysis followed the same criteria. Heat maps (Fig. 1D) and volcano maps (Fig. 1C) for DEG clustering can be generated using the same R software package.

The DAVID online database tool can be used in the KEGG enrichment analysis of the dataset GSE109476 DEGs. Cellular components (CC), molecular functions (MF), and biological processes (BP) are included in the graphene oxide category. Enrichment of the IL-17 signaling pathway in response to cytokine-cytokine receptor interactions can be demonstrated by KEGG analysis (Fig. 1G). A path map of the first 10 up-regulated and down-regulated DEGs can be created using the GOplot and ggplot2 packages in R (Fig. 1E and F).

Interactions between mRNA and lncRNA were predicted using the starBase database, focusing on associations such as has-miR-211-5p and BRD4. Visualization of interaction sites was provided (Fig. 1H and I).

In order to explore gene co-expression, scatter plots related to SOD1, JUN, PTPN11 and other genes could be drawn, data set refinement was carried out, and Pearson correlation coefficient could be calculated (Fig. 1J-N). Expression levels of PTPN11 can be illustrated in tumor and non-cancerous tissues (Fig. 1O).

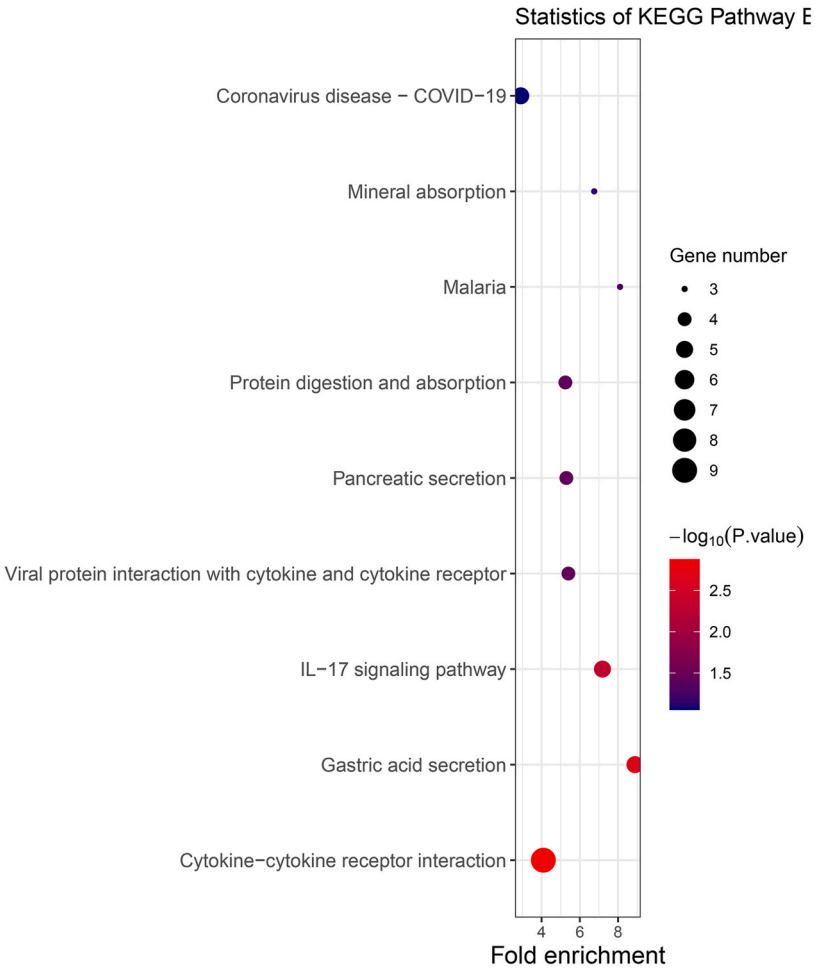

(g)

```
mRNA  :  5'  UGUUUGCUUGUGCAAAAGGGAA  3'
                |  :  :    :||   |||||||
miRNA  :  3'  UCCGCUUCCUACUGUUUCCCUU  5'
```

(b)

```
LncRNA  :  5'  AGAACCCAUUUCUCAAGGGAGA  3'
                 |  :  :    :||   |||||||
 miRNA  :  3'  UCCGCUUCCUACUGUUUCCCUU  5'
```

(c)

Fig. 1. (*continued*).

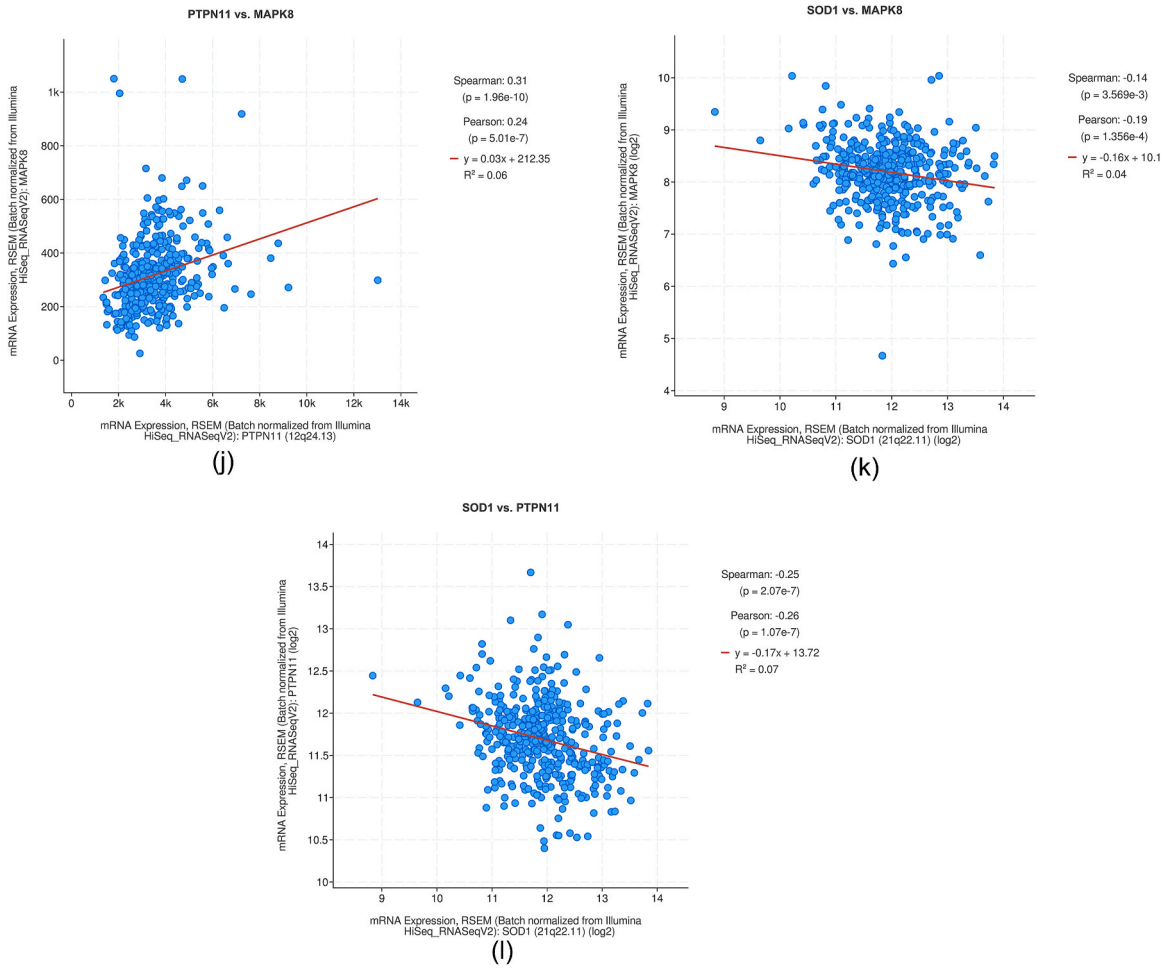

Fig. 1. (*continued*).

3.2. SHP2 inhibits CAR-T cell cytotoxicity against MGC-803 cells

A xenograft tumor model in nude mice demonstrated that, contrasted with the SHP2-NC group, the SHP2-NC + CAR-T group had significantly reduced tumor volume and weight. There were no notable dissimilarities between the SHP2-mimic group and the SHP2-mimic + CAR-T group, implying that SHP2 overexpression inhibits CAR-T cell cytotoxicity on MGC-803 cells (Fig. 2).

3.3. SHP2 inhibits ROS/JNK/P53 axis protein expression in MGC-803 cells

Western blot results indicated decreased *p*-SHP2 levels and increased *p*-JNK, NOX4, and P53 levels in the SHP2-NC + CAR-T group contrasted with the SHP2-NC group. There were no notable dissimilarities between the SHP2-mimic group and the SHP2-mimic + CAR-T group, suggesting that SHP2 overexpression suppresses the ROS/JNK/P53 axis (Fig. 3A).

3.4. lncRNA SNHG18 inhibits miR-211-5p

Initially, Q-PCR results revealed a notable increase in lncRNA SNHG18 expression and compared with the SHP2-NC group, the expression of miR-211-5p was reduced in the SHP2-mimic group. Addition of PHPS1 reversed these changes, normalizing their expressions. As can be seen from the dual luciferase reporter gene detection, the luminescence intensity of SNHG18-wt in the miR-211-5p simulated group was lower than that of the NC group. Compared with SNHG18-mut, there was no significant difference between the two groups (Fig. 3B and C).

3.5. lncRNA SNHG18 promotes CAR-T cell exhaustion and apoptosis

Western blot analysis showed that relative expression levels of BRD4, PD-L1, IDO1 and Bax in the lncRNA snhg18 inhibitor group

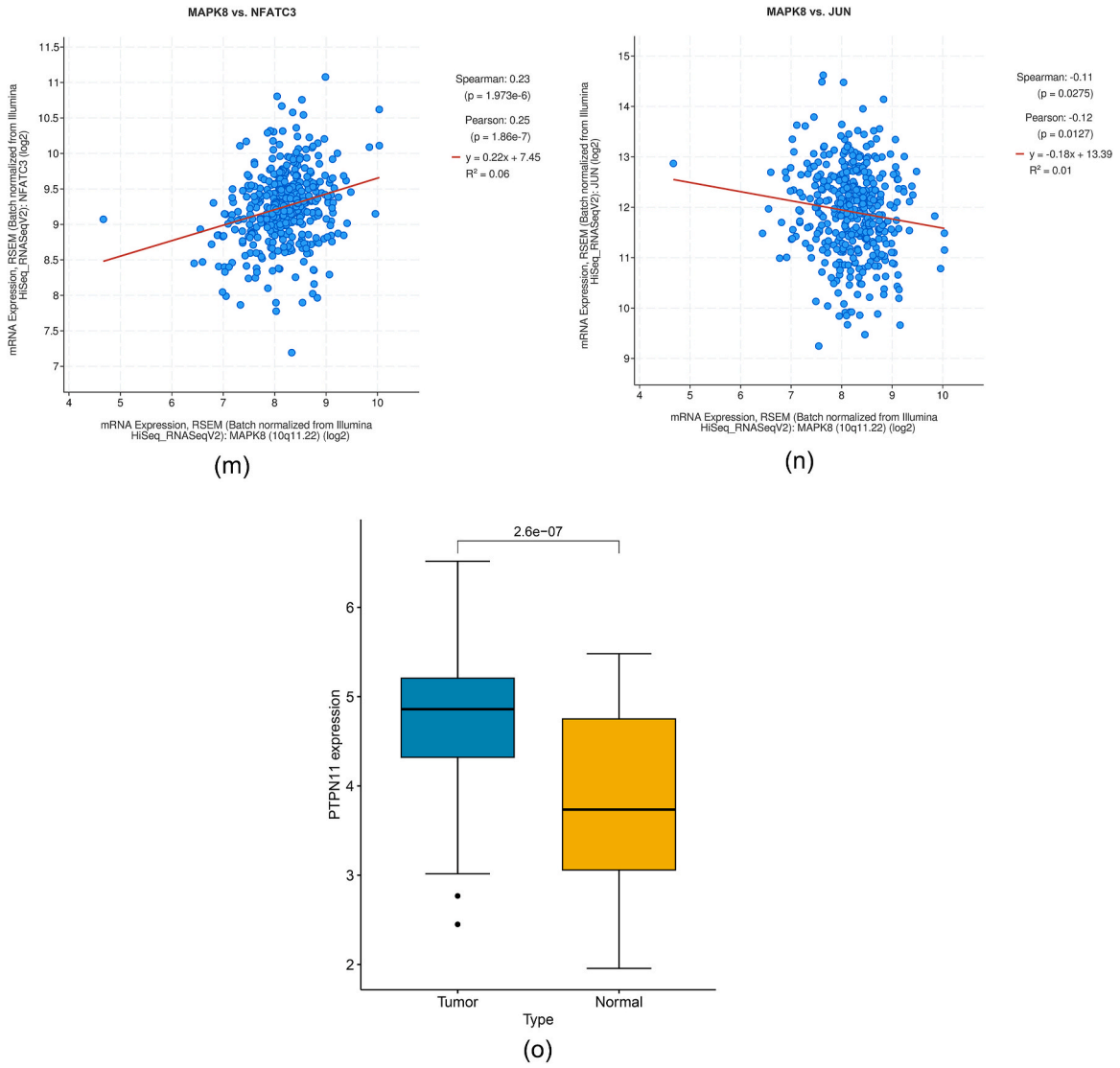

Fig. 1. (*continued*).

were lower than those in the NC group. On the contrary, protein levels increased more significantly in both lncRNA SNHG18 sh-RNA + mir-211-5p inhibitor group and NC + mir-211-5p inhibitor group, with no significant difference between the two groups. The same effect could be observed on the lncRNA SNHG18 sh-RNA + miR-211-5p-mimic group and the NC + miR-211-5p-mimic group (Fig. 4). These findings suggest that the depletion of CAR T cells may benefit from lncRNA SNHG18.

3.6. lncRNA SNHG18 inhibits MGC-803 cell proliferation and migration

Wound healing assay results showed a significantly reduced cell gap in the lncRNA SNHG18-inhibitor group contrasted with the NC group. In contrast, there was a marked increase in the intercellular space, No significant difference was found in lncRNA SNHG18 sh-RNA + Mir-211-5p mimic group, NC + Mir-211-5p mimic group, ncRNA SNHG18 sh-RNA + Mir-211-5p inhibitor group and NC + mir group -211-5p inhibitor group.Transwell assay results demonstrated a significant increase in migrating cells in the lncRNA SNHG18-inhibitor group contrasted with the NC group, while significant reductions were observed in both NC + miR-211-5p-inhibitor and lncRNA SNHG18 sh-RNA + miR-211-5p-inhibitor groups, with no notable dissimilarities between them; the same pattern was observed for the NC + miR-211-5p-mimic and lncRNA SNHG18 sh-RNA + miR-211-5p-mimic groups (Fig. 5A and B). These findings indicate that lncRNA SNHG18 inhibits MGC-803 cell migration capacity.

The CCK8 assay results revealed that at 72 h, Compared with the NC group, OD value in lncRNA snhg18 inhibitor group was increased. Conversely, OD values significantly decreased, with no notable differences between the groups of NC + miR-211-5p-inhibitor and lncRNA SNHG18 sh-RNA + miR-211-5p-inhibitor; the same pattern was observed for the NC + miR-211-5p-mimic and

(a)

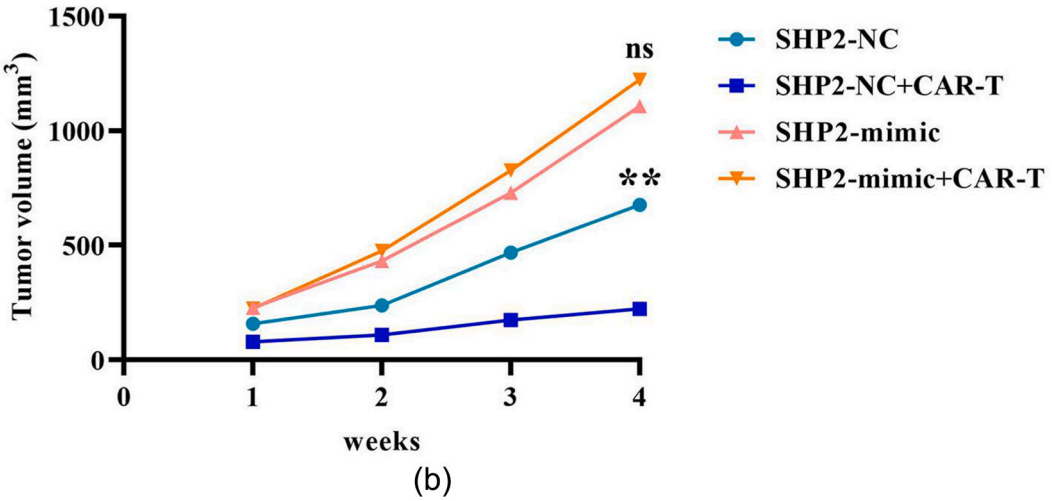

(b)

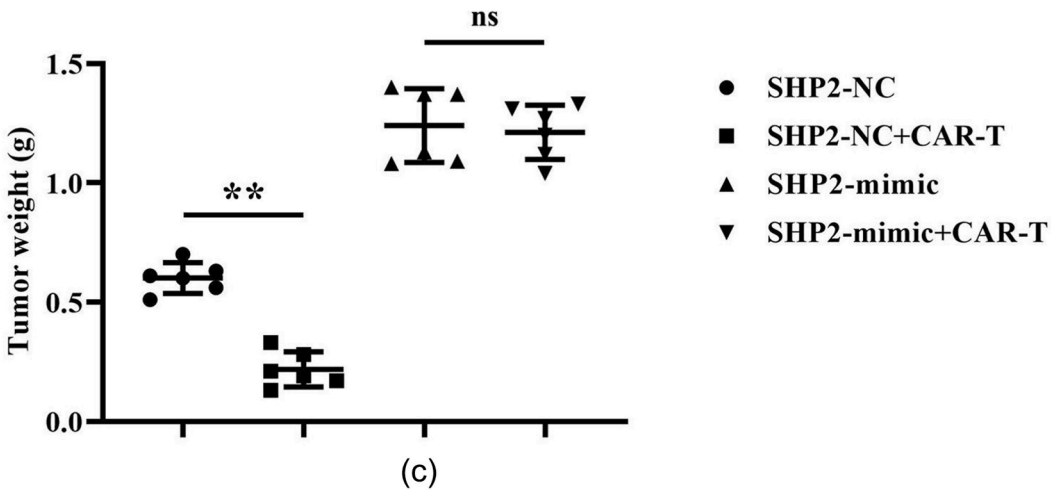

(c)

Fig. 2. SHP2 can inhibit the killing effect of CAR-T cells on MGC-803 cells.
A: Diagram of the subcutaneous tumor implantation experiment in nude mice; B: Tumor volume chart; C: Histogram of tumor weight.**P < 0.01;^{ns}P>0.05.

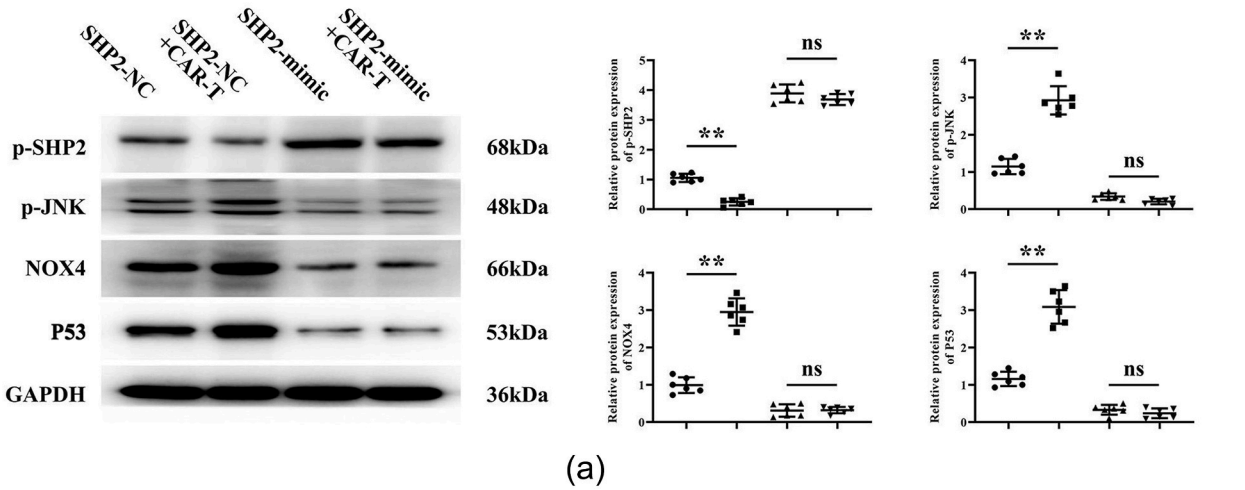

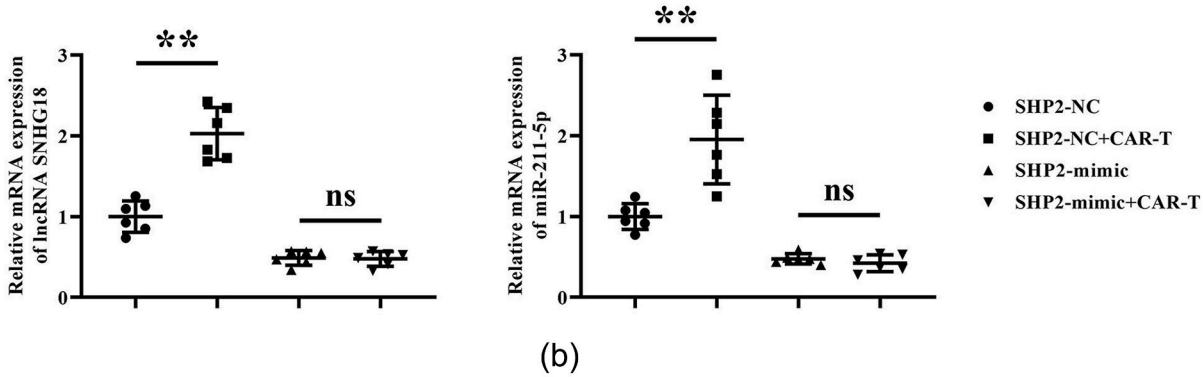

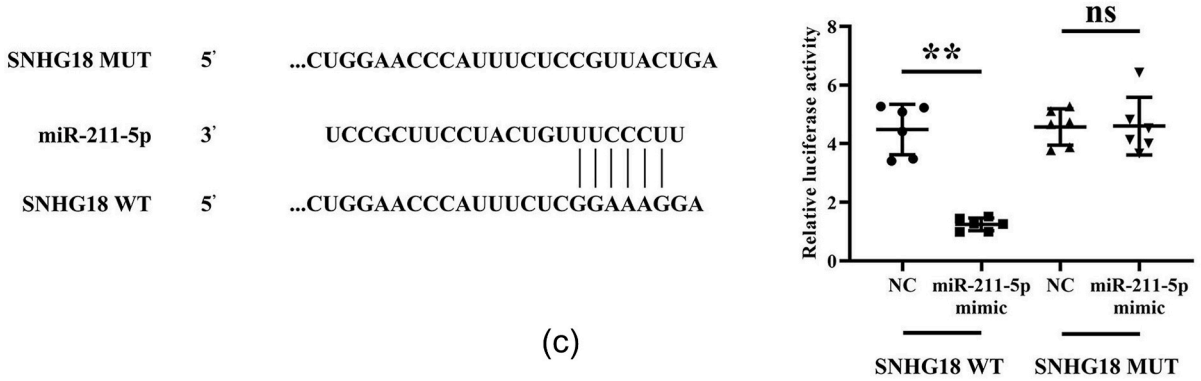

Fig. 3. SHP2 Can Mediate the Expression of ROS/JNK/P53 Axis Related Proteins in MGC-803 Cells and lncRNA SNHG18 Can Specifically Target Inhibit miR-211-5p Expression.
A: Western blot strips for *p*-SHP2, *p*-JNK, P53, and NOX4 and statistical graph of relative protein expression; B: Q-PCR detection of the expression of SNHG18 and miR-211-5p; C: Statistical results of the Dual-Luciferase reporter assay.**P < 0.01;^{ns}P>0.05.

lncRNA SNHG18 sh-RNA + miR-211-5p-mimic groups (Fig. 5C). This suggests that lncRNA SNHG18 inhibits the proliferative ability of MGC-803 cells.

Altogether, these findings indicate that in gastric cancer cells, SHP2 modulates the ROS/JNK/NFAT4 signaling pathway, which induces lncRNA SNHG18, Gastric cancer growth and metastasis can be driven by CAR-T cells via the miR-211-5p/BRD4 axis (Fig. 6).

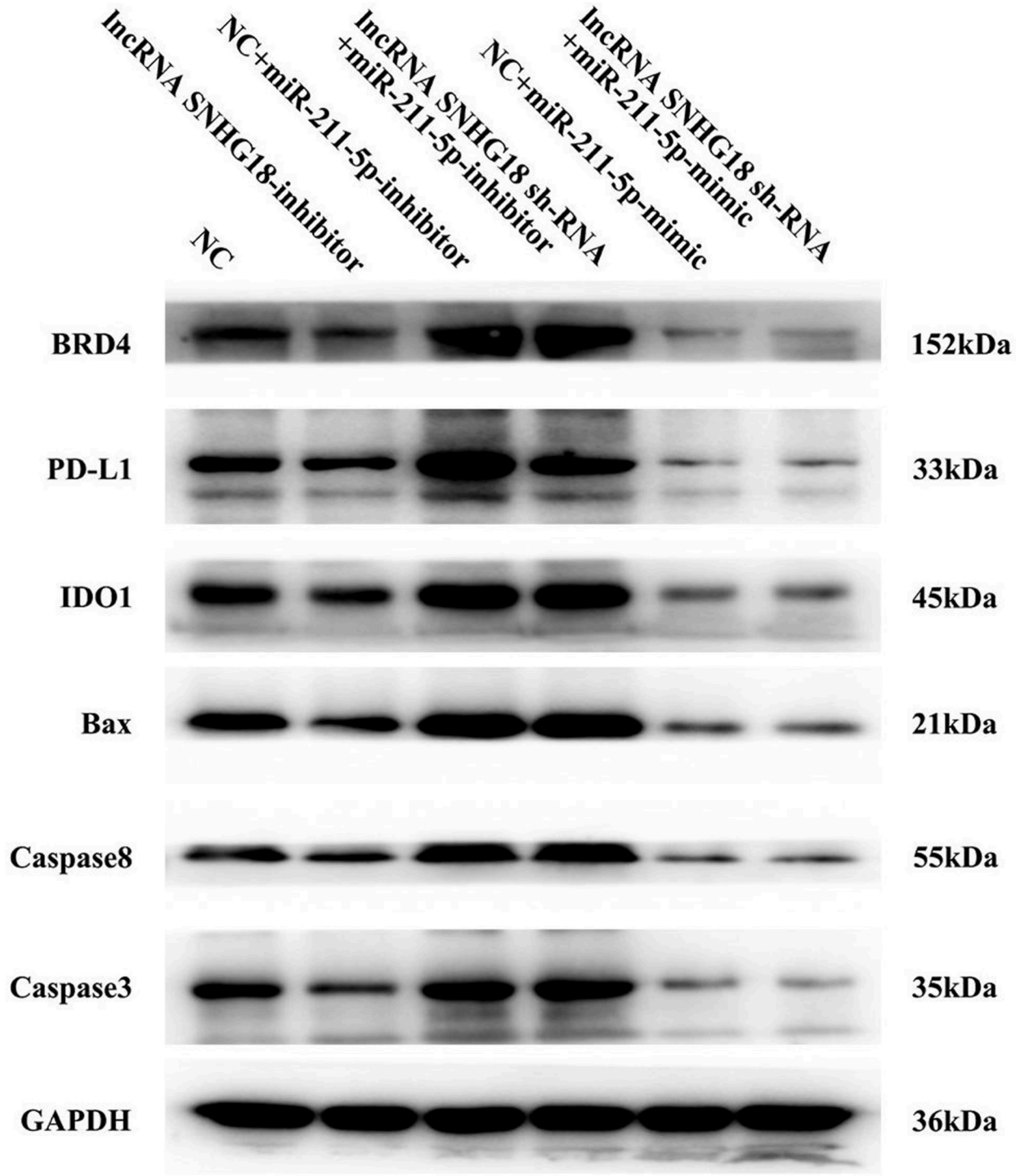

Fig. 4. lncRNA SNHG18 Can Promote CAR-T Cell Exhaustion and Apoptosis.
A: Protein strips of BRD4, PD-L1, IDO1, Caspase-3, Caspase-8, and Bax; B: Statistical graph of relative protein expression levels of BRD4, PD-L1, IDO1, Caspase-3, Caspase-8, and Bax.**$P < 0.01$;$^{ns}P>0.05$.

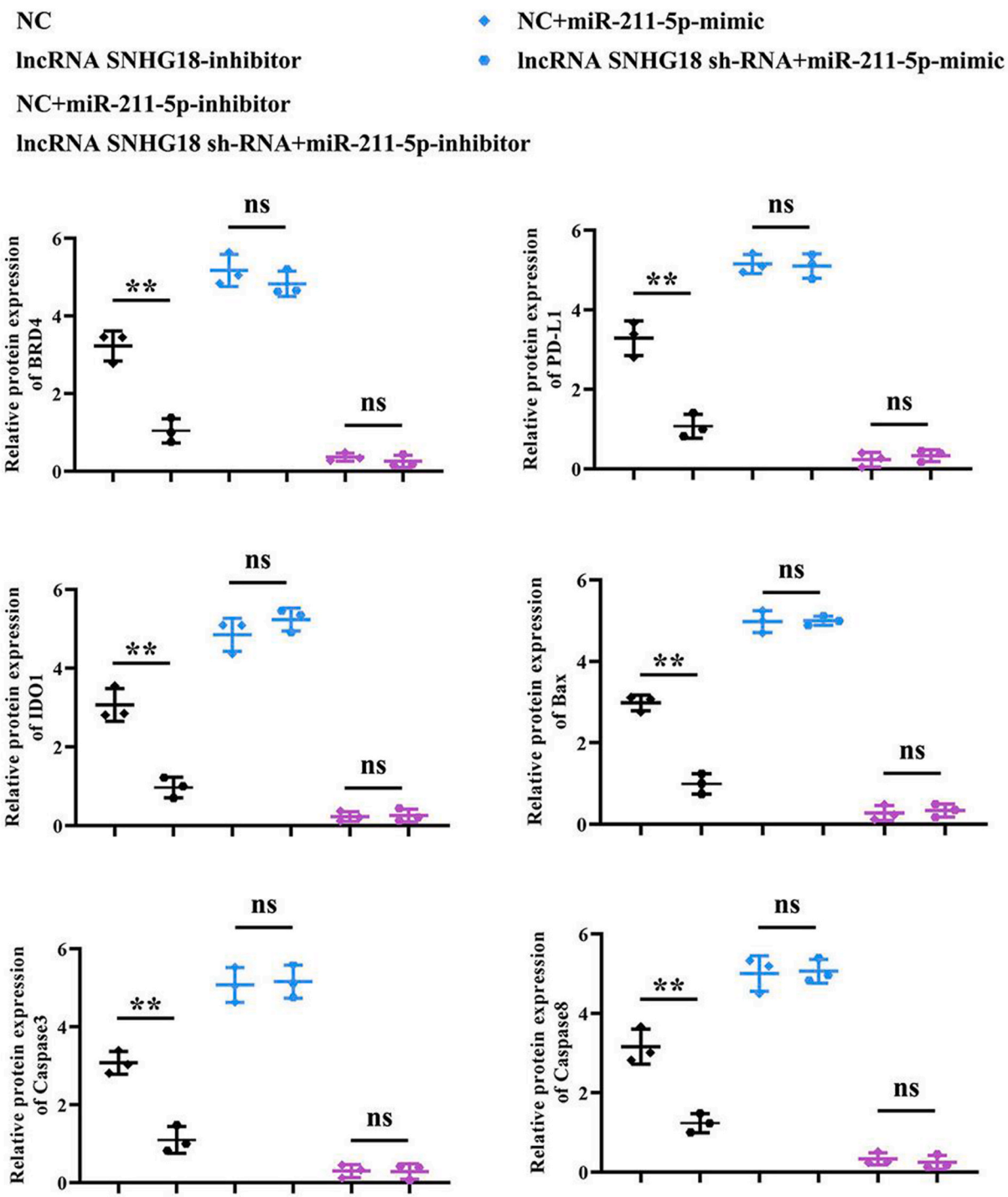

Fig. 4. (*continued*).

4. Discussion

Gastric adenocarcinoma refers to stomach cancer. This malignancy begins in the epithelial cells of the gastric mucosa. This cancer is very common worldwide, which also causes death. The prevalence of gastric cancer differs significantly across various regions, with particularly high rates in Asia, notably East Asia, including countries like Japan and Korea. Cancer cells can be identified and attacked by exploiting the patient's own immune system [11]. Immunotherapy has shown promise in the various cancer 's treatment, including

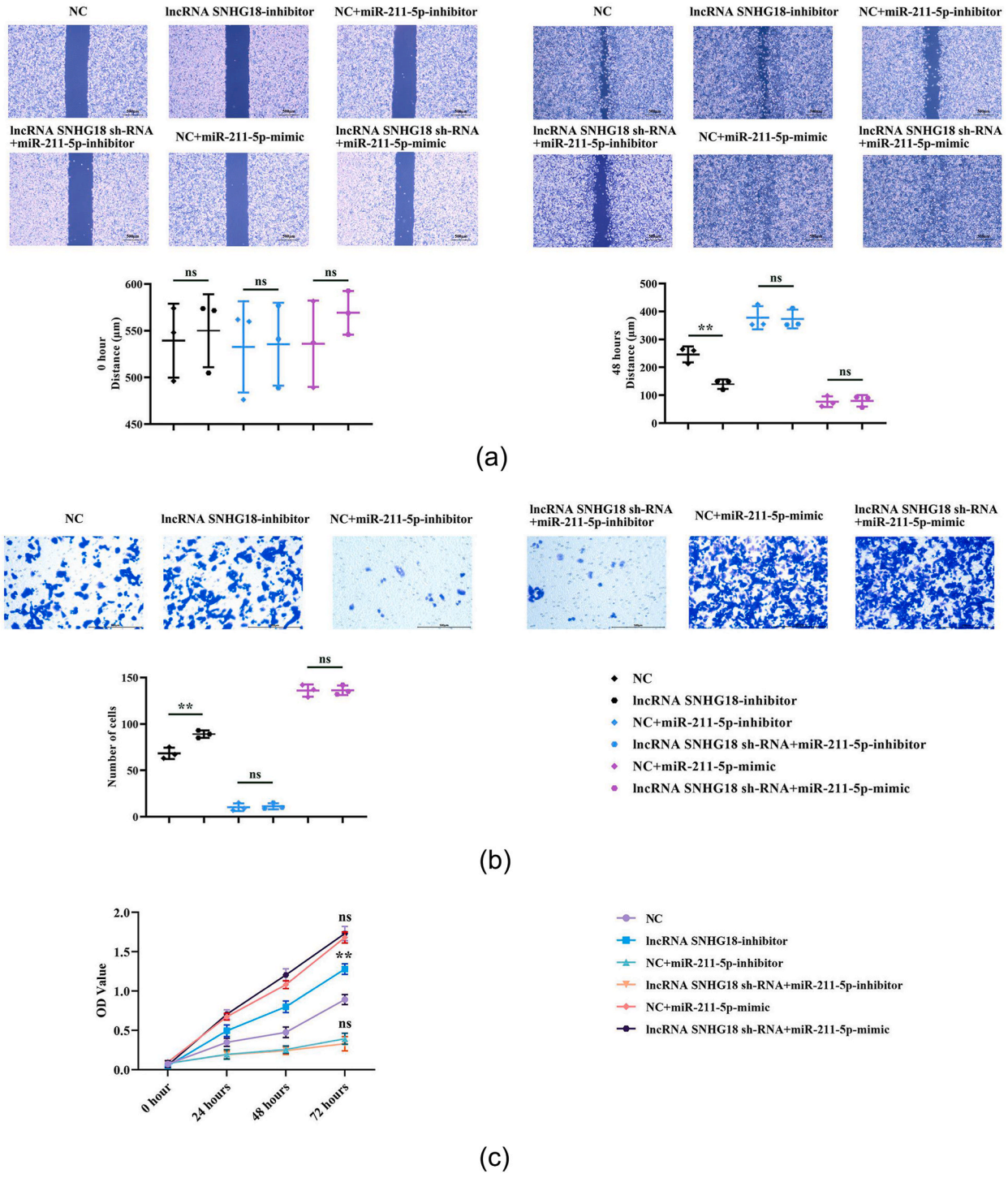

Fig. 5. lncRNA SNHG18 Can Inhibit the Proliferation and Migration of MGC-803 Cells.
A: Diagram and cell gap statistical graph of the wound-healing assay; B: Diagram of transwell assay and statistical graph of the number of migrating cells; C: CCK8 assay result graph.**P < 0.01;^{ns}P>0.05.

lung cancer, melanoma, kidney cancer, and bladder cancer. Given the outstanding clinical efficacy of CAR-T cell therapy in hematologic malignancies, the importance of CAR-T cell therapy for solid tumors, including gastric cancer, has been increasingly recognized [12,13]. Therefore, CAR-T cell therapy offers a broad prospect for this type of malignancy.

Within the microenvironment of gastric cancer, various biophysical and biochemical changes occur, including local hypoxia and

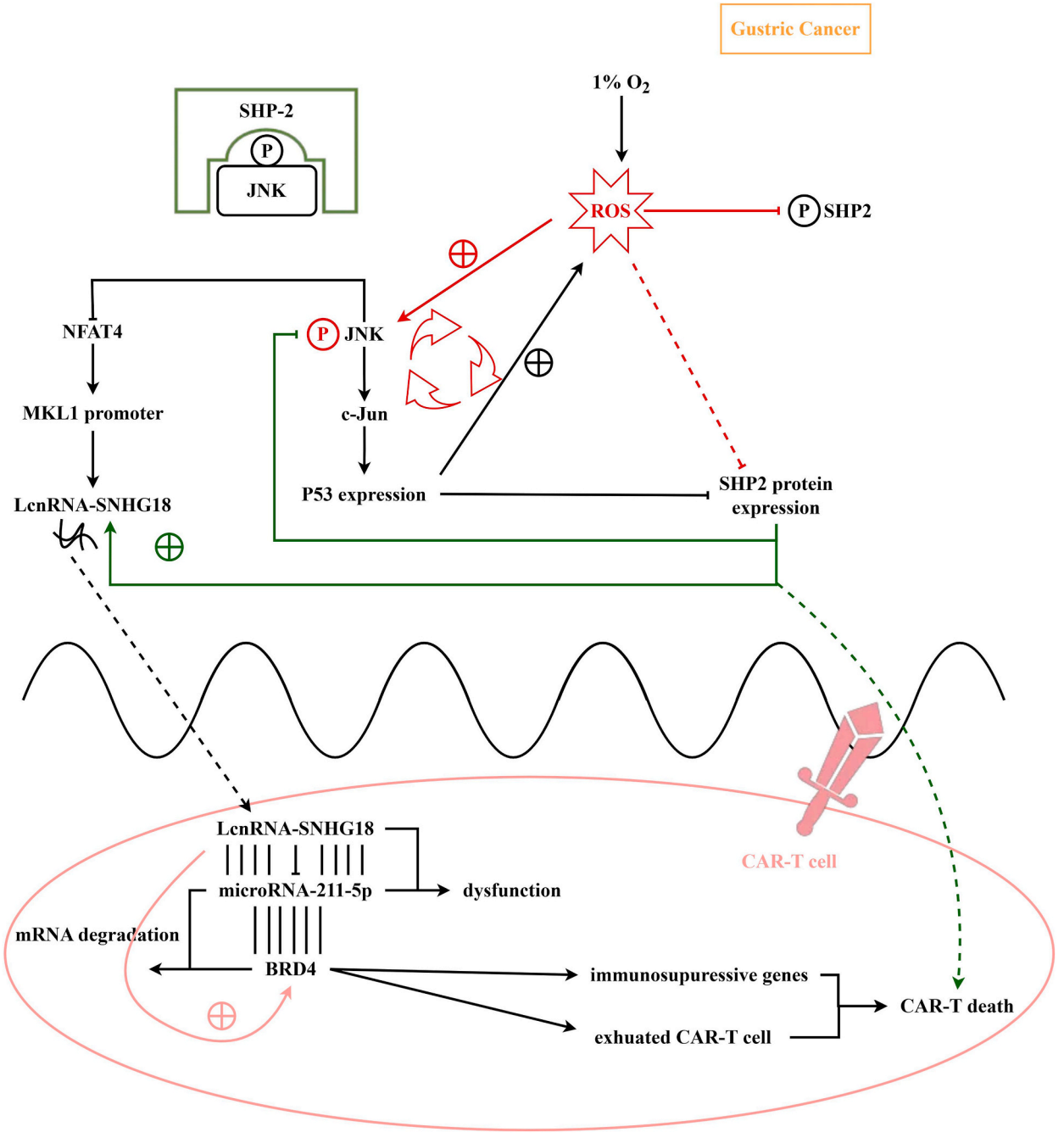

Fig. 6. SHP2 in gastric cancer cells mediates the ROS/JNK/NFAT4 signaling pathway, inducing lncRNA SNHG18 to drive growth and metastasis through the miR-211-5p/BRD4 axis in CAR-T cells.

increases in reactive oxygen species (ROS). Rapid tumor growth may exceed the capacity of existing blood supply, leading to insufficient blood flow to certain areas within the tumor and resulting in hypoxia. In the tumor microenvironment, which is typically characterized by hypoxia, tumor invasion and metastasis can be promoted through multiple mechanisms. If ROS levels are elevated, cell function can be affected by the activation of several cell signaling pathways, such as the c-Jun N-terminal kinase (JNK) pathway [14]. Under normal physiological conditions, JNK responds to cellular stress, cytokines, and growth factors. The p53 protein, an important tumor suppressor known as "the guardian of the cell" [15,16]. JNK can directly affect p53, promoting its phosphorylation. Activation of the p53 protein typically requires phosphorylation at multiple sites, which aids in releasing it from cellular inhibitors, stabilizing it, and translocating it to the nucleus to activate downstream gene expression. Moreover, in order to promote ROS production, the transcription of apoptosis-related genes can be activated by p53.During apoptosis, mitochondrial integrity may be

compromised, leading to increased ROS production. Research has shown that ROS and P53 can inhibit SHP2, and SHP2 can dephosphorylate JNK. In this study, The cytotoxic effect of CAR T cells on gastric cancer can be observed by overexpression of SHP2 Furthermore, the research also found that SHP2 can inhibit the expression of *p*-JNK, NOX4, and P53.

NFAT proteins are dephosphorylated upon calcium signal activation,the nucleus can be transferred from the cytoplasm and the expression of target genes can be regulated, typically under the control of the calcium-dependent phosphatase calcineurin. JNK can indirectly inhibit the activation state of NFAT by maintaining a pro-inflammatory environment, specifically regulating NFAT4 (or NFATc3) by signals from calcium and inositol 1,4,5-triphosphate (IP3)-dependent release [17,18]. MKL1 (Megakaryoblastic Leukemia 1, also known as MAL or MRTF-A) is a co-transcription factor for serum response factor (SRF) and is particularly important for processes involving the cytoskeleton, cell adhesion, and cell migration. MKL1 regulates its activity through binding states with actin monomers: it binds to G-actin (globular-actin) when G-actin is abundant, preventing MKL1 from relocating to the nucleus; when G-actin is depleted, indicating changes in cytoskeletal structure, The nuclear binding to SRF can be transported through the release of MKL1, thus activating target gene expression [19–21]. As the downstream target gene of MKL1, the up-regulation of BRD4 by miR-211-5p can be inhibited in NSCLC cells. In this study, the expression of NFAT4 and MKL1 can be promoted by SHP2, and SNHG18 was found to specifically inhibit miR-211-5p.

BRD4 is an epigenetic regulator that binds to acetylated histone tails, impacting chromatin structure and gene transcription. In many cancer types, BRD4 is associated with the continuous proliferation, survival, and exacerbation of tumor cells, and can lead to the exhaustion of CAR-T cells. As a cell surface protein, PD-L1(programmed cell death ligand 1) can bind to PD-1(programmed cell death protein 1). As an immunosuppressive receptor, PD-1 is present on T cells when binding is carried out by PD-L1 and PD-1, T cell activity is inhibited, diminishing their aggressiveness against tumor cells. Tumor cells often evade the host's immune attack by overexpressing PD-L1. The enzyme involved in tryptophan metabolism refers to IDO1(indoleamine 2, 3-dioxygenase 1), and kynuridine can be derived from the catalytic conversion of tryptophan. IDO1 is highly expressed in many tumors' microenvironments and creates an immunosuppressive environment by impairing T cell responses and promoting regulatory T cell production. Thus, inhibiting IDO1 activity is considered to improve anti-tumor immune responses. As a transcriptional regulator, BRD4 may directly or indirectly modulate the expression of PD-L1 and IDO1 [22]. In this study, we found that inhibiting lncRNA SNHG18 suppresses the expression of BRD4, PD-L1, IDO1, Bax, Caspase-3, and Caspase-8 in CAR-T cells, and promotes migration and proliferation abilities of MGC-803 cells.

In conclusion, ROS/JNK/NFAT4 signaling pathway can be mediated by SHP2, and lncRNA SNHG18 driving gastric cancer growth and metastasis can be induced by CAR T cells via the miR-211-5p/BRD4 axis. New targets and therapeutic approaches can be provided for the treatment of gastric cancer.

Funding

None.

Data availability

The datasets used and analyzed during the current study available from the corresponding author on reasonable request.

Ethics statement

This study has been approved by the Ethics Committee of Hebei University Hospital.(HDFYLL-KGCP-2024-091)

CRediT authorship contribution statement

Lin An: Writing – original draft, Supervision, Project administration, Methodology, Investigation, Funding acquisition. **Yue Huo:** Writing – original draft, Validation, Resources, Funding acquisition, Formal analysis, Data curation. **Na Xiao:** Project administration, Methodology, Conceptualization. **Shenyong Su:** Supervision, Software, Project administration, Methodology. **Kunjie Wang:** Writing – review & editing, Writing – original draft, Funding acquisition, Formal analysis, Data curation, Conceptualization.

Declaration of competing interest

The authors declare that they have no known competing financial interests or personal relationships that could have appeared to influence the work reported in this paper.

Acknowledgements

None.

References

[1] C. RöCKEN, Predictive biomarkers in gastric cancer, J. Cancer Res. Clin. Oncol. 149 (1) (2023) 467–481.

[2] A.P. Thrift, H.B. EL-Serag, Burden of gastric cancer, Clin. Gastroenterol. Hepatol. : the official clinical practice journal of the American Gastroenterological Association 18 (3) (2020) 534–542.
[3] J. Machlowska, J. Baj, M. Sitarz, et al., Gastric cancer: epidemiology, risk factors, classification, genomic characteristics and treatment strategies, Int. J. Mol. Sci. 21 (11) (2020) 4012.
[4] S. Zhang, D. Ren, H. Hou, et al., M-CSF secreted by gastric cancer cells exacerbates the progression of gastric cancer by increasing the expression of SHP2 in tumor-associated macrophages, Aging 15 (24) (2023) 15525–15534.
[5] S. Li, X. Wang, Q. Li, et al., Role of SHP2/PTPN11 in the occurrence and prognosis of cancer: a systematic review and meta-analysis, Oncol. Lett. 25 (1) (2023) 19.
[6] Y. Nagamura, M. Miyazaki, Y. Nagano, et al., SHP2 as a potential therapeutic target in diffuse-type gastric carcinoma addicted to receptor tyrosine kinase signaling, Cancers 13 (17) (2021) 4309.
[7] D. Bębnowska, E. Grywalska, P. Niedźwiedzka-Rystwej, et al., CAR-T cell therapy-an overview of targets in gastric cancer, J. Clin. Med. 9 (6) (2020) 1894.
[8] X. Jin, Z. Liu, D. Yang, et al., Recent progress and future perspectives of immunotherapy in advanced gastric cancer, Front. Immunol. 13 (2022) 948647.
[9] Q. Feng, B. Sun, T. Xue, et al., Advances in CAR T-cell therapy in bile duct, pancreatic, and gastric cancers, Front. Immunol. 13 (2022) 1025608.
[10] R. Zhao, Y. Cui, Y. Zheng, et al., Human hyaluronidase PH20 potentiates the antitumor activities of mesothelin-specific CAR-T cells against gastric cancer, Front. Immunol. 12 (2021) 660488.
[11] J. Chen, Z. Xu, C. Hu, et al., Targeting CLDN18.2 in cancers of the gastrointestinal tract: new drugs and new indications, Front. Oncol. 13 (2023) 1132319.
[12] W. Zhao, L. Jia, M. Zhang, et al., The killing effect of novel bi-specific Trop2/PD-L1 CAR-T cell targeted gastric cancer, Am. J. Cancer Res. 9 (8) (2019) 1846–1856.
[13] C. Chen, Y.M. Gu, F. Zhang, et al., Construction of PD1/CD28 chimeric-switch receptor enhances anti-tumor ability of c-Met CAR-T in gastric cancer, OncoImmunology 10 (1) (2021) 1901434.
[14] L. Wang, C. Wang, Z. Tao, et al., Curcumin derivative WZ35 inhibits tumor cell growth via ROS-YAP-JNK signaling pathway in breast cancer, J. Exp. Clin. Cancer Res. : CR 38 (1) (2019) 460.
[15] J. Shi, X. Yang, Q. Kang, et al., JNK inhibitor IX restrains pancreatic cancer through p53 and p21, Front. Oncol. 12 (2022) 1006131.
[16] Z.Q. He, P.F. Huan, L. Wang, et al., Paeoniflorin ameliorates cognitive impairment in Parkinson's disease via JNK/p53 signaling, Metab. Brain Dis. 37 (4) (2022) 1057–1070.
[17] D. Pal, S. Dutta, D.P. Iyer, et al., Identification of PAX6 and NFAT4 as the transcriptional regulators of the long noncoding RNA Mrhl in neuronal progenitors, Mol. Cell Biol. 42 (11) (2022) e0003622.
[18] P. Zhang, K. Li, Z. Wang, et al., Transient receptor potential vanilloid type 4 (TRPV4) promotes tumorigenesis via NFAT4 activation in nasopharyngeal carcinoma, Front. Mol. Biosci. 9 (2022) 1064366.
[19] P. Gao, P. Gao, J. Zhao, et al., MKL1 cooperates with p38MAPK to promote vascular senescence, inflammation, and abdominal aortic aneurysm, Redox Biol. 41 (2021) 101903.
[20] T. Wu, N. Li, Q. Zhang, et al., MKL1 fuels ROS-induced proliferation of vascular smooth muscle cells by modulating FOXM1 transcription, Redox Biol. 59 (2023) 102586.
[21] Z. Liu, J. Sun, C. Li, et al., MKL1 regulates hepatocellular carcinoma cell proliferation, migration and apoptosis via the COMPASS complex and NF-κB signaling, BMC Cancer 21 (1) (2021) 1184.
[22] C.Q. Tian, L. Chen, H.D. Chen, et al., Inhibition of the BET family reduces its new target gene Ido1 expression and the production of L-kynurenine, Cell Death Dis. 10 (8) (2019) 557.